Journal of Hepatocellular Carcinoma

Dovepress
Taylor & Francis Group

Open Access Full Text Article

ORIGINAL RESEARCH

The U-Shaped Association Between Remnant Cholesterol and Postoperative Survival in Hepatocellular Carcinoma: Development and Validation of an Interpretable Machine Learning Model

Gao-Min Liu[1,2], Jia-Peng Liao[1,2], Ji-Wei Xu[1,2]

[1]Department of Hepatobiliary Surgery, Meizhou Clinical Institute of Shantou University Medical College, Meizhou, 514000, People's Republic of China; [2]Department of Hepatobiliary Surgery, Meizhou People's Hospital, Meizhou, 514000, People's Republic of China

Correspondence: Ji-Wei Xu, Department of Hepatobiliary Surgery, Meizhou People's Hospital, No. 38 Huangtang Road, Meizhou, 514000, People's Republic of China, Tel +0086-13823832715, Email javeeht@163.com

Background and Objectives: The prognostic role of remnant cholesterol (RC) in hepatocellular carcinoma (HCC) remains unexplored. This study aimed to investigate the association between RC and overall survival (OS) in HCC patients after hepatectomy and to develop a robust prognostic model.

Materials and Methods: 439 HCC patients who underwent curative hepatectomy were retrospectively analyzed. RC was calculated as total cholesterol minus (HDL-c + LDL-c). To specifically evaluate the potential nonlinear relationship, the association between RC and OS was assessed using restricted cubic splines (RCS) in addition to Cox regression and subgroup analyses. A machine learning approach employing nine algorithms was used to develop a prognostic model, with model interpretability achieved using SHapley Additive exPlanations (SHAP). An online predictive tool was subsequently deployed.

Results: A significant U-shaped relationship between RC and OS (P for non-linearity = 0.013) was identified, with the lowest risk observed at approximately 1.04 mmol/L. Both too low and too high RC levels were independent predictors of worse OS. Among the machine learning models, XGBoost demonstrated superior and consistent performance for predicting 1-, 3-, and 5-year OS. SHAP analysis confirmed RC as a key predictive feature, alongside TNM stage and tumor characteristics. An interactive web-based tool was successfully implemented for clinical use.

Conclusion: RC demonstrates a novel U-shaped association with HCC postoperative survival in an Asian HBV-endemic cohort, underscoring its role as a significant biomarker reflecting metabolic imbalance. The developed machine learning model, which integrates RC, provides accurate, interpretable, and individualized risk assessment, offering a valuable tool for clinical prognostication and potential guidance for personalized management strategies.

Keywords: hepatocellular carcinoma, remnant cholesterol, machine learning, survival, U-shaped relationship

Introduction

Hepatocellular carcinoma (HCC) remains one of the most lethal cancers worldwide.[1] The majority of patients are diagnosed at an intermediate or advanced stage and can only receive palliative treatments such as transarterial or systemic therapy. Curative treatment options, including hepatectomy, liver transplantation, and radiotherapy, are applicable to only a small proportion of HCC patients. Moreover, postoperative recurrence and metastasis continue to pose major obstacles to improving clinical outcomes.[2] Consequently, the overall survival of HCC remains suboptimal. Numerous studies have sought to identify additional risk factors to facilitate patient stratification and prolong prognosis.[3,4]

Received: 22 September 2025
Accepted: 25 November 2025
Published: 1 December 2025

Hepatocytes play a crucial role in maintaining systemic cholesterol homeostasis and serve as the primary site of cholesterol metabolism. Studies have shown that in various tumor cells, including HCC, the activation of oncogenic pathways or inactivation of tumor suppressor pathways during cancer progression can lead to dysregulated cholesterol metabolism, characterized by enhanced synthesis and uptake to meet increased energy and biosynthetic demands.[5] Many studies have observed abnormal cholesterol accumulation in HCC tissues, which is not a passive process but actively contributes to malignant progression.[6,7] A deeper understanding of the mechanisms and clinical implications of cholesterol in HCC development is of great importance.

In recent years, with the widespread use of statins, research focus has gradually shifted to triglyceride-rich lipoproteins.[8] HDL-c (high-density lipoproteins-c) has demonstrated significant value in early prediction and risk stratification of HCC, and has been identified as a novel biomarker for predicting HCC.[9] Furthermore, in patients receiving immunotherapy, higher baseline levels of serum HDL-c or ApoA1 are associated with improved survival.[10] Lipoprotein-related metabolites such as VLDL (very low-density lipoprotein) and LDL (low-density lipoprotein) are significantly altered upon the onset of HCC. Nine lipid-related metabolites have been identified as potential diagnostic markers for HCC, six of which exhibit high discriminatory power in distinguishing between cirrhotic and healthy tissues.[11] Additionally, the LCAT/HDL-c axis has been recognized as a potential therapeutic target in HCC by modulating cholesterol homeostasis to suppress hepatocarcinogenesis, suggesting that both LCAT and HDL-c may serve as prognostic and therapeutic biomarkers.[12] Current evidence indicates that HDL-c is a reliable predictive marker, particularly for NAFLD-HCC risk stratification, while triglycerides and lipoprotein metabolites hold potential value in diagnosis and prognosis.

Residual cholesterol (RC) refers to the cholesterol content of triglyceride-rich lipoprotein remnants derived from the degradation of triglycerides or during the transformation of lipoproteins. RC includes cholesterol components other than HDL and LDL, such as VLDL, intermediate-density lipoproteins IDL, and chylomicron remnants. Previous research on RC has primarily focused on cardiovascular disease, diabetes, and related complications such as ischemic stroke.[13–15] However, in recent years, its role in cancer has garnered increasing attention. For example, studies have found that RC can effectively predict postoperative survival in breast cancer.[16] Preliminary evidence suggests that elevated RC levels are generally associated with an increased risk of mortality from cardiovascular disease, yet may correlate with a reduced overall mortality risk in certain cancers, including liver and gastric cancers.[17] However, these associations require further validation, and the relationship between RC and postoperative prognosis in HCC patients after resection has not been investigated.

Therefore, this study aimed to investigate the association between RC and overall survival in HCC patients undergoing hepatectomy, in order to provide more accurate guidance for individualized treatment and survival prediction, and to improve risk stratification and management.

Materials and Methods

Study Population

We retrospectively analyzed 439 patients with hepatocellular carcinoma (HCC) who underwent hepatectomy as their initial treatment at Meizhou People's Hospital between May 2011 and February 2024. This study was conducted in accordance with the Declaration of Helsinki and was approved by the Ethics Committee of Meizhou People's Hospital (approval no. 2023-C-95). As patient consent was waived by the Ethics Committee of Meizhou People's Hospital for this retrospective study, all patient data were anonymized and maintained with confidentiality to protect privacy.

Inclusion and Exclusion Criteria

Inclusion criteria were as follows: (I) hepatectomy as the primary treatment; (II) pathological confirmation of HCC; (III) availability of biochemical blood test results within one week prior to surgery; (IV) complete clinicopathological data, including RC levels and follow-up information.

Exclusion criteria included: (I) history of multiple primary malignancies; (II) receipt of any prior antitumor therapy such as chemotherapy, radiotherapy, or interventional treatment. A flowchart illustrating patient selection is provided in Supplementary Figure 1.

Data Collection

Collected data encompassed: 1) Demographics: age, sex, body mass index (BMI), background liver disease (hepatitis, cirrhosis, portal hypertension), and Child-Pugh score. 2) Preoperative blood parameters: albumin (ALB), alanine aminotransferase (ALT), alpha-fetoprotein (AFP), total bilirubin (TBIL), triglycerides (TG), total cholesterol (TC), high-density lipoprotein cholesterol (HDL-c), low-density lipoprotein cholesterol (LDL-c), glutamyl transpeptidase (GGT), and hepatitis B surface antigen (HBsAg). 3) Surgical details: intraoperative blood loss, surgical approach (open/laparoscopic), extent of resection (major/minor), and anatomic resection status. 4) Tumor characteristics: size, number, capsule integrity, vascular invasion, microvascular invasion (MVI), and TNM stage (8th edition). 5) Follow-up: overall survival (OS) was determined from the date of surgery until death or last follow-up. The final follow-up date was February 7, 2025, providing a minimum of one year of potential follow-up for the last patient included (operated on in February 2024). Pathological reviews were conducted independently by two pathologists to ensure diagnostic consistency.

Calculation of RC

RC was calculated as the cholesterol content of triglyceride-rich lipoproteins, including very low-density lipoprotein (VLDL), intermediate-density lipoprotein (IDL), and chylomicron remnants. The formula applied was:RC=Total Cholesterol - (HDL-c + LDL-c). Patients were stratified into high- and low-RC groups based on an optimal cut-off value determined using the "survminer" R package. The statistical power of RC was calculated with "powerSurvEpi" R package.

Subgroup and Sensitivity Analyses

To ensure the robustness of our findings, comprehensive subgroup analyses were performed based on age (≤60/>60 years), sex, TNM stage (I+II/III+IV), tumor number (single/multiple), MVI status, surgical approach, and other key clinicopathological variables. Interaction effects were tested using likelihood ratio tests.

Sensitivity analyses included: 1) 1:1 Propensity score matching (PSM) to further balance baseline characteristics between high- and low-RC groups. 2) Inverse probability of treatment weighting (IPTW) based on propensity scores to minimize potential confounding and simulate a randomized study context. 3) Cut-off point shift analyses by varying the RC threshold by ±5% to assess the stability of the association. 4) Exclusion of early mortality cases by repeating analyses after removing patients who died within 6 and 12 months post-surgery. 5) Winsorization of continuous variables at the 1st and 99th percentiles to minimize the influence of outliers.

Dose–Response Analysis and Nonlinear Relationship Assessment

The dose–response correlation between RC and overall survival was analyzed using restricted cubic splines (RCS) with four knots. The linear model for RC was also compared against the RCS model using likelihood ratio tests. In cases of a nonlinear relationship, potential threshold effects were identified by systematically testing all possible inflection points and selecting the most probable values. A piecewise Cox proportional hazards regression model was then applied to evaluate the correlation between RC and survival, stratified by the identified inflection point.

Machine Learning Modeling

Given the non-linear relationship between RC and survival identified in preliminary analyses, a machine learning approach was employed to develop a robust prognostic model. The dataset was randomly partitioned into training (70%) and testing (30%) sets using the createDataPartition function from the R caret package (version 6.0–94). To ensure reproducibility, a fixed random seed was set using set.seed (123) prior to partitioning. To handle the high-dimensional data and enhance model performance, we first selected variables with a significance level of $P < 0.05$ from univariate Cox regression analysis. These variables were subsequently included for further modeling. Multicollinearity was assessed using variance inflation factors (VIF), and variables with VIF > 10 were excluded to ensure model stability.

We developed and compared nine machine learning models for survival prediction: Least Absolute Shrinkage and Selection Operator (LASSO) -Cox, CoxBoost, survival support vector machine (Survival-SVM), random survival forest (RSF), gradient boosting machine (GBM), extreme gradient boosting (XGBoost), super principal components (SuperPC),

partial least squares Cox regression (plsRcox), and stepwise Cox regression (stepCox). Each model underwent hyperparameter tuning and tenfold cross-validation. Model performance was comprehensively evaluated using several metrics: the time-dependent area under the receiver operating characteristic curve (AUC), the mean concordance index (C-index), calibration curves, and decision curve analysis (DCA).[18] These methods were employed to assess both the predictive accuracy and clinical utility of the developed models. To enhance the interpretability of the optimal model, SHapley Additive exPlanations (SHAP) analysis was further utilized to quantify the contribution and direction of each feature toward the prediction, thereby providing both global and individual-level interpretations of the model's output. The optimal model was deployed as an interactive web-based tool to facilitate clinical application.

Statistical Analysis

All analyses were performed using R software (v4.3.1). Continuous variables were expressed as mean ± standard deviation or median [interquartile range], and categorical variables as counts (percentages). Group comparisons utilized Student's *t*-test, Mann–Whitney *U*-test, χ^2-test, or Fisher's exact test as appropriate. Survival analyses were conducted using Kaplan–Meier curves and Log rank tests. Univariate and multivariate Cox proportional hazards models were employed to identify prognostic factors. A two-sided p-value < 0.05 was considered statistically significant.

Results

Baseline Clinicopathological Characteristics

A total of 439 HCC patients were included. The high- and low-RC groups showed significant differences in diabetes prevalence, Child-Pugh score, albumin levels, ALT, TG, TC, LDL-c, and presence of vascular invasion (all p < 0.05). No significant differences were observed in other baseline characteristics, including TNM stage (Table 1).

Prognostic Value of RC

The cut-off point of RC was set as 0.62 mmol/L. Univariate Cox analysis indicated that high RC was associated with worse OS (HR = 1.54, 95% CI: 1.07–2.23, p = 0.021). Multivariate analysis confirmed RC as an independent prognostic factor (HR = 1.52, 95% CI: 1.04–2.23, p = 0.032), along with tumor multiplicity, advanced TNM stage, and low ALI (all p < 0.05) (Table 2). The statistical power of RC was 70.0% at α=0.05. Kaplan-Meier curves demonstrated significant

Table 1 Baseline Characteristics of Included 439 HCC Patients

Characteristics	Level	Overall	RC (HIGH=249)	RC (LOW=190)	P value
Age (mean (SD)) (Years)		58.10 (11.28)	57.86 (11.00)	58.41 (11.67)	0.616
Gender (%)	Male	390 (88.8)	223 (89.6)	167 (87.9)	0.081
	FeMale	49 (11.2)	26 (10.4)	23 (12.1)	0.693
BMI (median [IQR]) (Kg/m2)		390 (88.8)	223 (89.6)	167 (87.9)	
Hypertension (%)	No	354 (80.6)	198 (79.5)	156 (82.1)	0.577
	Yes	85 (19.4)	51 (20.5)	34 (17.9)	
Diabetes (%)	No	367 (83.6)	200 (80.3)	167 (87.9)	***0.046***
	Yes	72 (16.4)	49 (19.7)	23 (12.1)	
HBsAg (%)	Negative	77 (17.5)	47 (18.9)	30 (15.8)	0.474
	Positive	362 (82.5)	202 (81.1)	160 (84.2)	
Cirrhosis (%)	No	132 (30.1)	77 (30.9)	55 (28.9)	0.732
	Yes	307 (69.9)	172 (69.1)	135 (71.1)	
Portal hypertension (%)	No	344 (78.4)	201 (80.7)	143 (75.3)	0.208
	Yes	95 (21.6)	48 (19.3)	47 (24.7)	
Child-Pugh score (%)	5	301 (68.6)	183 (73.5)	118 (62.1)	***0.015***
	6	138 (31.4)	66 (26.5)	72 (37.9)	

(*Continued*)

Table 1 (Continued).

Characteristics	Level	Overall	RC (HIGH=249)	RC (LOW=190)	P value
AFP (median [IQR]) (ng/mL)		2551.58 (6158.59)	2584.28 (5707.42)	2508.72 (6719.40)	0.899
ALB (mean (SD)) (g/L)		40.68 (5.28)	41.28 (4.92)	39.90 (5.64)	***0.006***
TBIL (mean (SD)) (umol/L)		17.86 (13.22)	17.37 (11.84)	18.50 (14.83)	0.376
GGT (mean (SD)) (U/L)		112.46 (334.94)	129.87 (427.79)	89.65 (137.60)	0.213
ALT (mean (SD)) (U/L)		56.05 (81.46)	63.16 (97.33)	46.75 (52.86)	***0.036***
TG (mean (SD)) (mmol/L)		1.24 (1.13)	1.44 (1.42)	0.98 (0.41)	***<0.001***
TC (mean (SD)) (mmol/L)		4.81 (1.39)	5.25 (1.48)	4.24 (1.00)	***<0.001***
HDL-c (mean (SD)) (mmol/L)		1.43 (0.67)	1.47 (0.71)	1.39 (0.61)	0.238
LDL-c (mean (SD)) (mmol/L)		2.60 (0.90)	2.70 (0.91)	2.47 (0.88)	***0.009***
Tumor size (mean (SD)) (cm)		5.58 (3.30)	5.56 (3.30)	5.61 (3.30)	0.889
Tumor size (%)	<5	210 (47.8)	119 (47.8)	91 (47.9)	1.000
	≥5	229 (52.2)	130 (52.2)	99 (52.1)	
Tumor number (%)	Single	343 (78.1)	197 (79.1)	146 (76.8)	0.649
	Multiple	96 (21.9)	52 (20.9)	44 (23.2)	
Tumor Capsule (%)	Complete	382 (87.0)	223 (89.6)	159 (83.7)	0.095
	InComplete	57 (13.0)	26 (10.4)	31 (16.3)	
Vascular invasion (%)	No	338 (77.0)	182 (73.1)	156 (82.1)	***0.035***
	Yes	101 (23.0)	67 (26.9)	34 (17.9)	
MVI (%)	M0	280 (63.8)	165 (66.3)	115 (60.5)	0.247
	M1	88 (20.0)	43 (17.3)	45 (23.7)	
	M2	71 (16.2)	41 (16.5)	30 (15.8)	
Tumor Grade (%)	1	22 (5.0)	11 (4.4)	11 (5.8)	0.323
	2	291 (66.3)	174 (69.9)	117 (61.6)	
	3	117 (26.7)	60 (24.1)	57 (30.0)	
	4	9 (2.1)	4 (1.6)	5 (2.6)	
Anatomical resection (%)	No	195 (44.4)	115 (46.2)	80 (42.1)	0.450
	Yes	244 (55.6)	134 (53.8)	110 (57.9)	
Surgical approach (%)	Conversion	54 (12.3)	29 (11.6)	25 (13.2)	0.631
	Lapro	250 (56.9)	139 (55.8)	111 (58.4)	
	Open	135 (30.8)	81 (32.5)	54 (28.4)	
Major resection (%)	No	309 (70.4)	171 (68.7)	138 (72.6)	0.427
	Yes	130 (29.6)	78 (31.3)	52 (27.4)	
Intraoperative_bleeding (mean (SD)) (mL)		320.98 (475.06)	320.96 (485.69)	321.00 (462.03)	0.999
TNM stage (%)	I+II	333 (75.9)	191 (76.7)	142 (74.7)	0.715
	III+IV	106 (24.1)	58 (23.3)	48 (25.3)	

Notes: Bold P: P<0.05.

Abbreviations: ALB, albumin; ALT, alanine aminotransferase; AFP, alpha fetoprotein; ALI, advanced lung cancer inflammation index; BMI, body mass index; GGT, glutamyl transpeptidase; HDL-c, high-density lipoprotein cholesterol; HBsAg, hepatitis B surface antigen; LDL-c, low-density lipoprotein cholesterol; MVI, microvascular invasion; RC, remnant cholesterol; TBIL, total bilirubin; TC, total cholesterol; TG, triglycerides; TNM, tumor node metastasis classification.

survival stratification based on RC levels (Figure 1). Notably, the combination of RC and ALI significantly enhanced prognostic discrimination, particularly in early-stage (TNM I+II) patients and within the low ALI subgroup. Patients with RC^{low}-ALI^{low} exhibited the poorest survival outcomes, while those with RC^{high}-ALI^{high} demonstrated optimal survival. This synergistic prognostic effect was not observed in advanced-stage patients.

Subgroup and Sensitivity Analyses

Subgroup analyses consistently indicated that elevated RC was associated with worse prognosis across most patient subgroups (Figure 2). Sensitivity analyses-including PSM (the balance plot was showed in Supplementary Figure 2),

Table 2 Univariate and Multivariate Cox Proportional Hazards Analysis of Factors Associated with HCC OS

Characteristics	HR (Univariable)	HR (Multivariable)	HR (Final)
Age (years) (≤ 60 vs >60)	1.20 (0.82–1.74, p=0.354)		
Gender (Male vs Female)	1.29 (0.67–2.47, p=0.440)		
BMI (≥ 25 vs <25)	0.51 (0.28–0.90, p=0.021)	0.62 (0.35–1.12, p=0.115)	0.61 (0.34–1.10, p=0.099)
Hypertension (Yes vs No)	0.72 (0.43–1.23, p=0.231)		
Diabetes (Yes vs No)	0.63 (0.34–1.14, p=0.125)		
HBsAg (Positive vs Negative)	1.53 (0.86–2.73, p=0.149)		
Cirrhosis (Yes vs No)	0.90 (0.60–1.36, p=0.626)		
Portal_hypertension (Yes vs NO)	1.05 (0.68–1.61, p=0.824)		
Child-Pugh score (6 vs 5)	1.23 (0.84–1.80, p=0.296)		
AFP (ng/mL) (≤20 vs >20)	0.50 (0.34–0.75, p<0.001)	0.72 (0.48–1.09, p=0.120)	0.72 (0.48–1.08, p=0.113)
ALB (g/L) (≥35 vs <35)	0.94 (0.54–1.61, p=0.809)		
TBIL (umol/L) (≤ 17.1 vs >17.1)	1.41 (0.95–2.09, p=0.084)		
GGT (U/L) (≤60 vs >60)	0.90 (0.62–1.30, p=0.586)		
ALT (U/L) (≤ 40 vs >40)	0.96 (0.66–1.39, p=0.820)		
Size (cm) (≥ 5 vs <5)	2.36 (1.59–3.50, p<0.001)	1.23 (0.77–1.94, p=0.388)	
Tumor number (Single vs Multiple)	0.49 (0.33–0.72, p<0.001)	0.50 (0.34–0.75, p=0.001)	**0.52 (0.35–0.77, p=0.001)**
Tumor capsule (Incomplete vs Complete)	1.99 (1.27–3.13, p=0.003)	0.71 (0.41–1.24, p=0.228)	
Vascular invasion (Yes vs No)	2.51 (1.71–3.69, p<0.001)	0.90 (0.50–1.60, p=0.709)	
MVI (M1+M2 vs M0)	1.21 (0.83–1.76, p=0.311)		
Tumor grade (G3+4 vs G1+2)	1.44 (0.98–2.11, p=0.065)		
Major resection (Yes vs No)	2.17 (1.50–3.15, p<0.001)	1.35 (0.90–2.04, p=0.152)	1.42 (0.96–2.11, p=0.082)
Anatomical resection (Yes vs No)	1.37 (0.94–1.99, p=0.103)		
Surgical Approach (Open vs Lapro)	1.95 (1.35–2.83, p<0.001)	1.27 (0.85–1.91, p=0.239)	
Intraoperative bleeding (mL) (≤ 400 vs >400)	0.99 (0.64–1.52, p=0.948)		
ALI (Low vs High)	2.01 (1.38–2.91, p<0.001)	1.88 (1.27–2.77, p=0.002)	**1.87 (1.28–2.73, p=0.001)**
RC (Low vs High)	1.54 (1.07–2.23, p=0.021)	1.64 (1.10–2.45, p=0.016)	**1.52 (1.04–2.23, p=0.032)**
TNM Stage (III+IV vs I+II))	4.64 (3.20–6.74, p<0.001)	3.76 (2.09–6.76, p<0.001)	**3.68 (2.47–5.49, p<0.001)**

Note: Bold Hazard Ratio (HR) values indicate variables that were statistically significant (P < 0.05) in the final multivariable model.
Abbreviations: ALB, albumin; ALT, alanine aminotransferase; AFP, alpha fetoprotein; ALI, advanced lung cancer inflammation index; BMI, body mass index; GGT, glutamyl transpeptidase; HDL-c, high-density lipoprotein cholesterol; HBsAg, hepatitis B surface antigen; LDL-c, low-density lipoprotein cholesterol; MVI, microvascular invasion; RC, remnant cholesterol; TBIL, total bilirubin; TC, total cholesterol; TG, triglycerides; TNM, tumor node metastasis classification.

IPTW, and evaluations in clinically homogeneous cohorts-consistently supported the robustness of this association. However, threshold shift analyses (±5%) showed that the prognostic significance of RC was lost when the cut-off value was perturbed, suggesting a potential non-linear relationship with OS (Table 3).

To further explore this, RCS analysis was performed, which confirmed a non-linear association between RC and OS (P for non-linearity = 0.013) (Figure 3A). Model comparisons using likelihood ratio tests revealed superior fit of the nonlinear RCS specification compared to the linear model (χ^2 (1) = 5.17, p = 0.023), supporting the presence of nonlinear effects. The RC level associated with the minimal mortality risk was identified at 1.04 mmol/L (95% CI: 0.74–1.21 mmol/L), as determined by bootstrap resampling with 1000 replicates. The optimal RC range, within which the HR for OS remained below 1, was identified as 0.59–2.74 mmol/L. Although Kaplan-Meier curves suggested a trend toward improved -though not statistically significant-OS in patients within this optimal range (Figure 3B), subsequent piecewise Cox regression based on the 1.04 mmol/L threshold demonstrated divergent effects: 1) for RC < 1.04 mmol/L, lower RC was associated with increased risk of mortality (HR = 2.259, 95% CI: 1.012–5.041, P = 0.047); 2) for RC ≥ 1.04 mmol/L, lower RC emerged as a significant protective factor (HR = 0.716, 95% CI: 0.547–0.937, P = 0.015) (Table 3). Together, these findings reveal a significant U-shaped relationship between RC and OS, underscoring the importance of avoiding simplistic dichotomization in future predictive modeling.

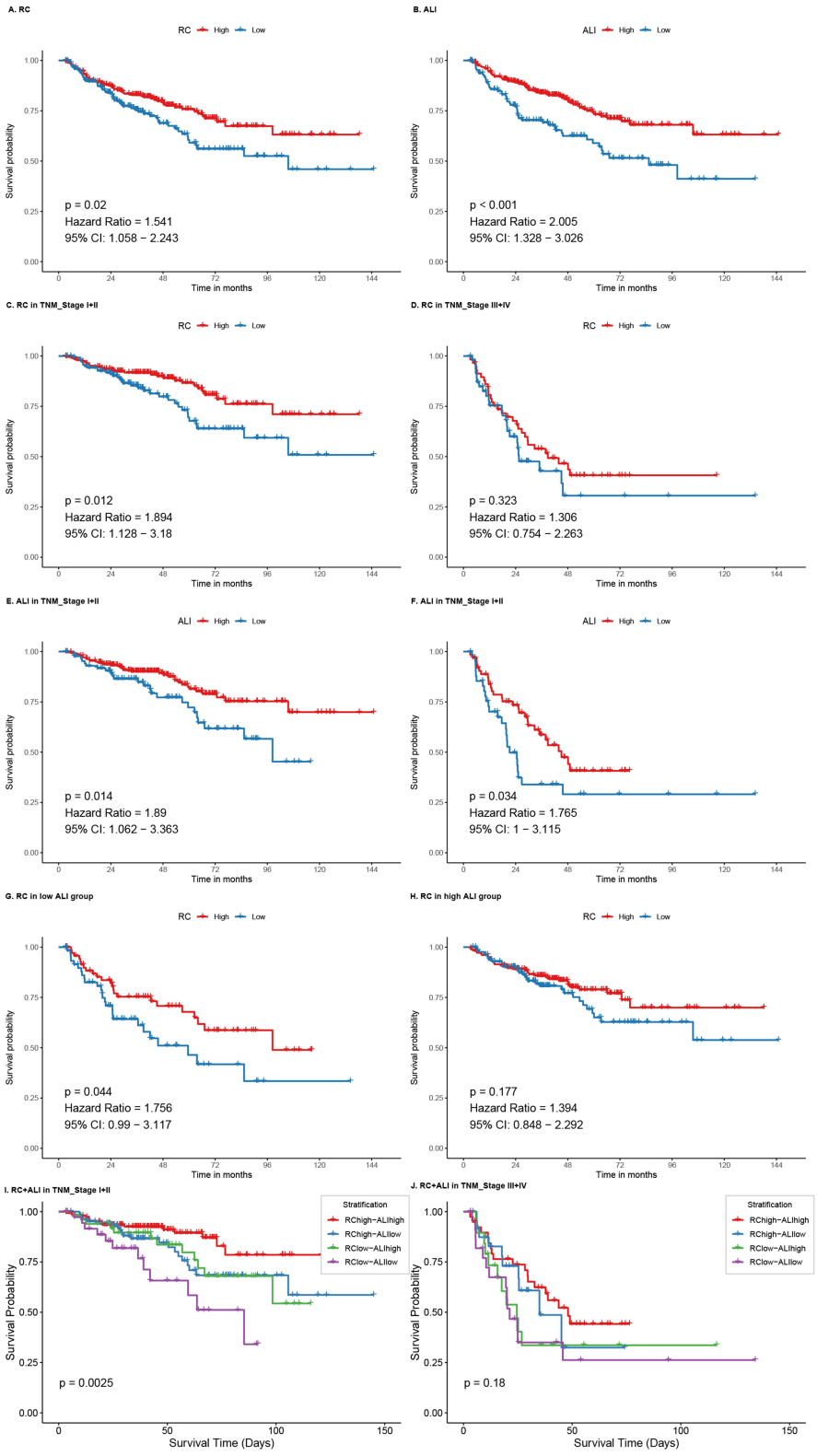

Figure 1 Kaplan-Meier survival curves stratified by RC, ALI, TNM stage, and their combinations. **(A)** Overall survival (OS) stratified by high vs low RC score. **(B)** OS stratified by high vs low ALI. **(C)** OS stratified by RC score in patients with TNM stage I–II HCC. **(D)** OS stratified by RC score in patients with TNM stage III–IV HCC. **(E)** OS stratified by ALI in patients with TNM stage I–II HCC. **(F)** OS stratified by ALI in patients with TNM stage III–IV HCC. **(G)** OS stratified by RC score in patients with low ALI. **(H)** OS stratified by RC score in patients with high ALI. **(I)** OS stratified by combined RC and ALI groups in patients with TNM stage I–II HCC. **(J)** OS stratified by combined RC and ALI groups in patients with TNM stage III–IV HCC.

https://doi.org/10.2147/JHC.S569292

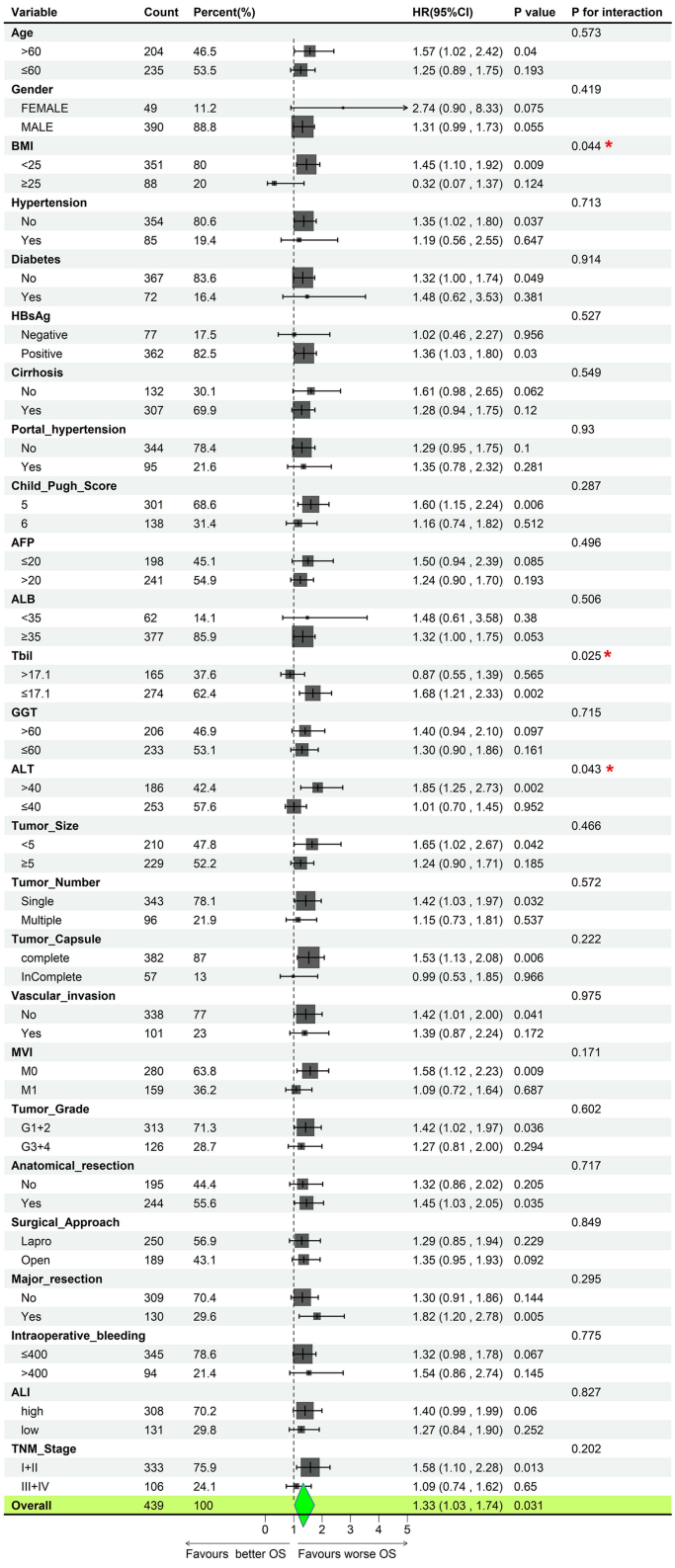

Figure 2 Forrest plot of the subgroup survival using univariate Cox regression analysis in HCC.

Table 3 Sensitivity Analyses of the Association Between Remnant Cholesterol and HCC Overall Survival After Hepatectomy

Analysis	HR (Low vs High RC)	P value
Crude analysis-hazard ratio (95% CI)	1.544 (1.069–2.232)	**0.021**
Multivariable analysis-hazard ratio (95% CI)	1.521 (1.042–2.229)	**0.032**
Sensitivity analysis		
Propensity-score analyses-hazard ratio (95% CI)		
With inverse probability weighting	1.539 (1.043–2.272)	**0.030**
Adjusted for propensity score	4.497 (1.016–2.206)	**0.042**
TNM stage I+II	1.918 (1.148–3.204)	**0.013**
Single tumor without MVI	2.422 (1.307–4.491)	**0.005**
Tumor grade 1+2 without MVI	2.010 (1.101–3.648)	**0.022**
Anatomical_resection with lower than 400 mL bleeding	1.757 (1.001–3.085)	**0.049**
Deceased within 6 months	1.564 (1.064–2.301)	**0.023**
Deceased within 12 months	1.962 (1.147–3.356)	**0.014**
Winsorization (retaining 99% data range)	1.505 (1.039–2.179)	**0.031**
+5% cut-off point shift	1.333 (0.920–1.930)	0.129
−5% cut-off point shift	1.329 (0.916–1.930)	0.134
Segmented cox model		
<1.04 mmol/L	2.259 (1.012–5.041)	**0.047**
>1.04mmol/L	0.716 (0.547–0.937)	**0.015**

Note: Bold P: P<0.05.
Abbreviations: remnant cholesterol; MVI, microvascular invasion; TNM, tumor node metastasis classification.

Machine Learning Model Development and Interpretation

Patients were subsequently divided into training and testing cohorts. The baseline characteristics between these two groups were well-balanced (Supplementary Table 1). The nine machine learning models exhibited varying predictive performance for 1-, 3-, and 5-year overall survival (Figure 4A and B). In the testing cohort, the AUC values for 1-year prediction were as follows: Lasso_Cox (0.728), SurvivalSVM (0.714), SuperPC (0.714), GBM (0.687), stepCox (0.669), CoxBoost (0.669), plsRcox (0.673), xgboost (0.671), and RSF (0.631). For 3-year prediction, the AUC values were:

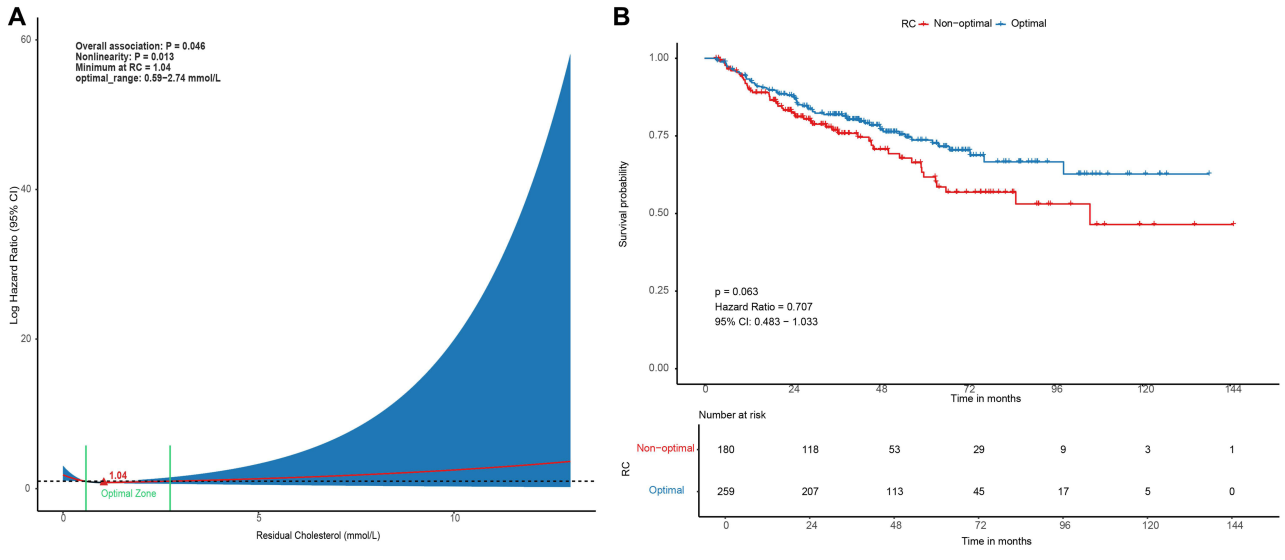

Figure 3 Association between RC levels and overall survival in hepatocellular carcinoma patients after hepatectomy. (**A**) Dose-response relationship between RC levels and log hazard ratio of mortality analyzed by restricted cubic splines (RCS). (**B**) Kaplan-Meier survival curves comparing patients with RC levels within the optimal range (0.59–2.74 mmol/L) versus those outside this range.

https://doi.org/10.2147/JHC.S569292

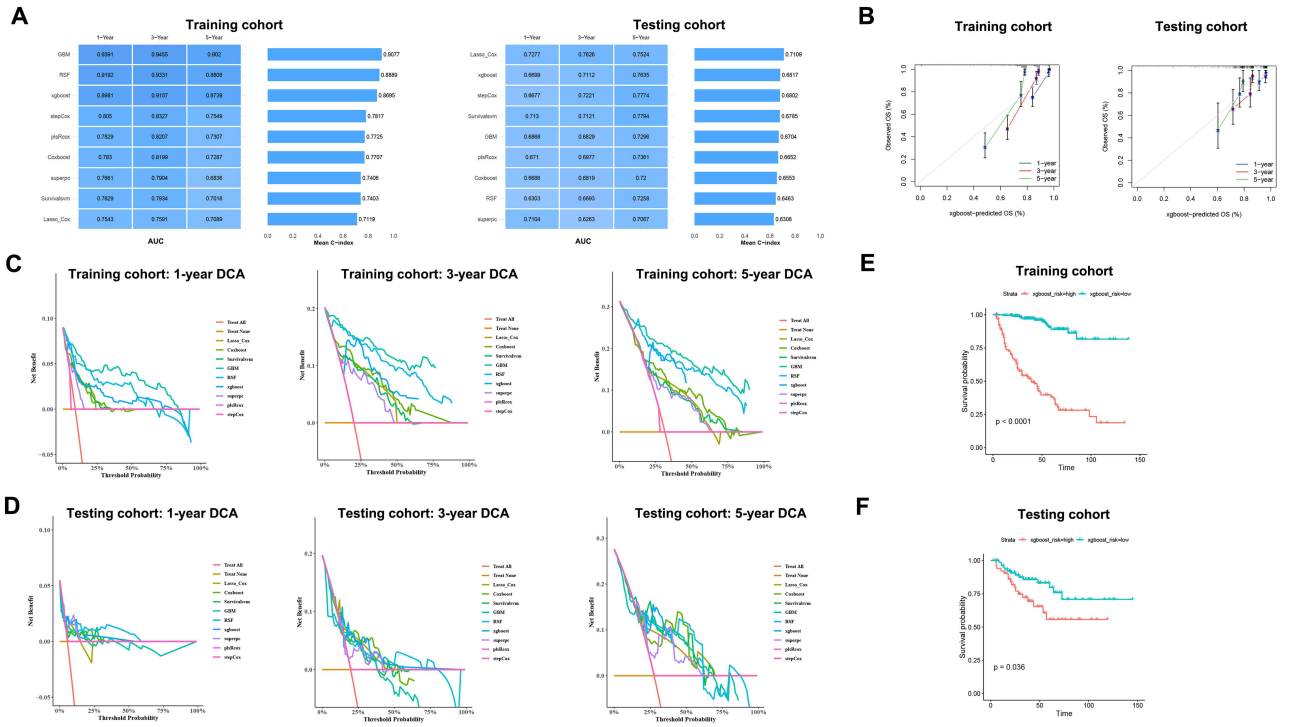

Figure 4 Performance and clinical utility of machine learning models for predicting overall survival in hepatocellular carcinoma patients. (**A**) Time-dependent AUC and mean C-index values of nine machine learning models for predicting 1-, 3-, and 5-year overall survival in the training and testing cohort. (**B**) Calibration curves of the XGBoost model for 1-, 3-, and 5-year survival prediction in the training and testing cohort, comparing predicted versus observed survival probabilities. (**C**) Decision curve analysis (DCA) showing the net benefit of each model across different threshold probabilities in the training cohort. (**D**) DCA showing the net benefit of each model across different threshold probabilities in the training and testing cohort. (**E**) Kaplan-Meier survival curves based on XGBoost-derived risk stratification (high vs low risk) in the training cohort. (**F**) Kaplan-Meier survival curves based on XGBoost-derived risk stratification in the testing cohort.

Lasso_Cox (0.724), xgboost (0.688), stepCox (0.689), GBM (0.665), SurvivalSVM (0.678), plsRcox (0.673), CoxBoost (0.657), RSF (0.649), and SuperPC (0.611). For 5-year prediction, the models achieved: Lasso_Cox (0.711), stepCox (0.708), xgboost (0.707), GBM (0.688), SurvivalSVM (0.698), plsRcox (0.678), RSF (0.668), CoxBoost (0.666), and SuperPC (0.639) (Figure 4B). Decision curve analysis demonstrated that all models provided higher net clinical benefit than the "treat all" or "treat none" strategies across a wide range of threshold probabilities at 1, 3, and 5 years. The calibration curves for the XGBoost model showed excellent agreement between predicted and observed outcomes in both training and testing sets (Figure 4C and D). Based on XGBoost-derived risk stratification, patients in both training and testing sets were categorized into high- and low-risk groups. Survival curve analysis revealed highly significant differences between these groups in the training set ($p < 0.0001$) (Figure 4E). Similarly, in the testing set, the XGBoost model maintained significant discriminative ability, with a statistically notable separation in survival outcomes between high- and low-risk groups ($p = 0.036$) (Figure 4F). These findings further validate the effectiveness and robustness of the XGBoost model in predicting post-operative survival risk in patients with hepatocellular carcinoma.

Given its consistent and high performance across all evaluation metrics and time points, the XGBoost model was identified as the optimal predictive tool tested for subsequent application.

Interpretability Analysis

SHAP analyses were employed to elucidate both global and individual prediction mechanisms of the optimal XGBoost model.

The SHAP summary plot (Beeswarm plot, Figure 5A) illustrates the overall impact and direction of each feature on model predictions. Red and blue colors indicate high and low feature values, respectively. The horizontal dispersion of points reflects the magnitude of a feature's contribution, with values farther from zero exerting stronger effects on the output. As shown in the feature importance ranking (Figure 5B), TNM stage (III+IV), RC, tumor number, ALI level, tumor size, AFP level, major resection, vascular invasion, surgical approach, and tumor capsule integrity were identified

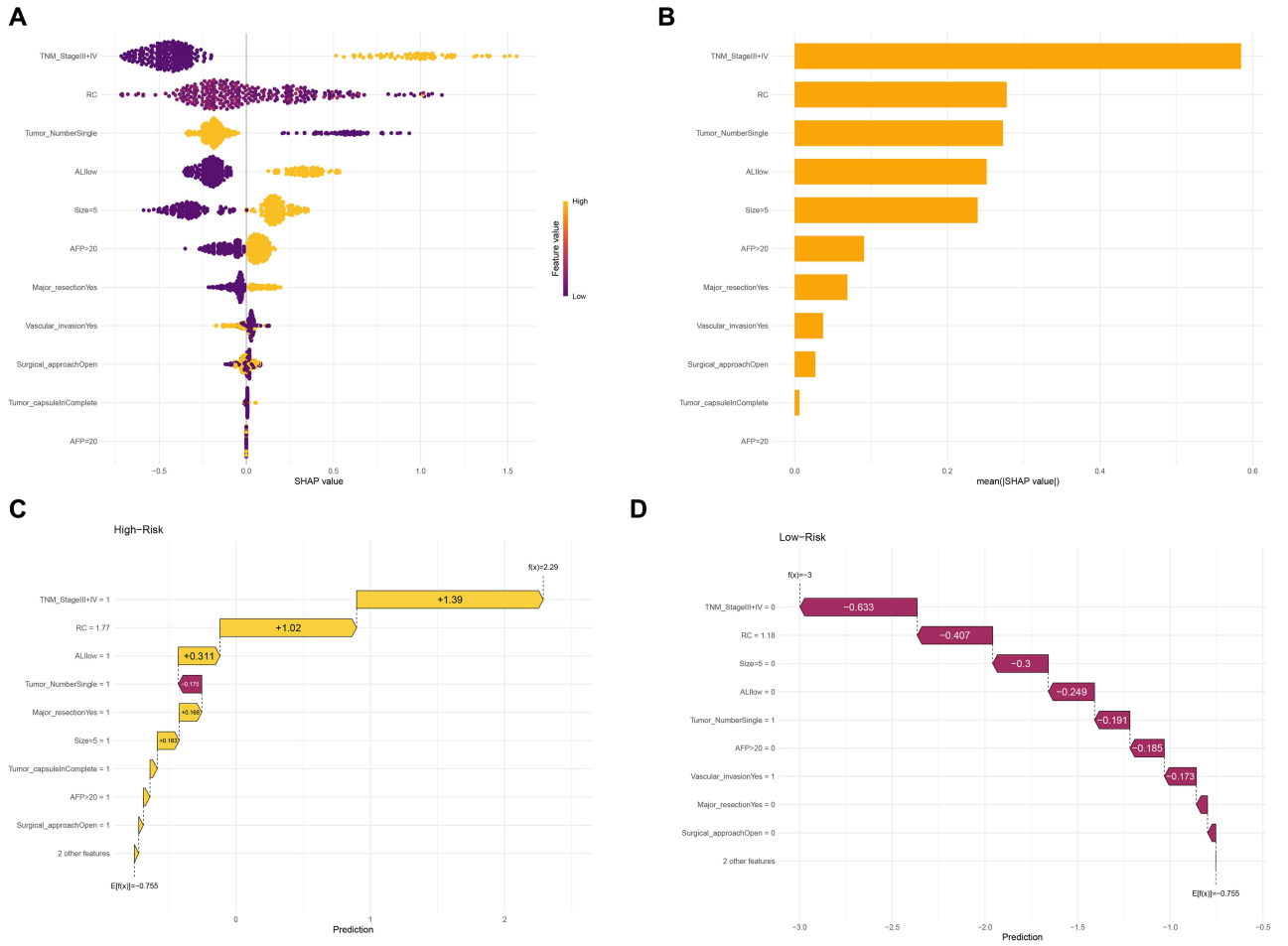

Figure 5 Interpretability analysis of the XGBoost model using SHapley Additive exPlanations (SHAP). **(A)** SHAP feature importance plot, showing the mean absolute SHAP value for each feature, which represents its overall contribution to the model's predictions. TNM_StageIII+IV, RC, and Tumor_NumberSingle were identified as the top three most influential features. **(B)** SHAP summary (beeswarm) plot, displaying the distribution of SHAP values for each feature. Each point represents a patient. The color indicates the feature value (red: high, blue: low), and the horizontal position shows the impact on the prediction (positive SHAP value increases risk, negative decreases risk). **(C)** SHAP waterfall plot explaining the prediction for a representative high-risk patient (predicted risk score: 289). **(D)** SHAP waterfall plot explaining the prediction for a representative low-risk patient (predicted risk score: 113).

as the most influential predictors. Among these, advanced TNM stage, elevated RC, multiple tumors, low ALI, larger tumor size, and AFP > 20 ng/mL were associated with increased risk of mortality.

SHAP waterfall plots were used to illustrate patient-specific risk contributors. For example: in a high-risk patient (Predicted risk score: 289), advanced TNM stage (III+IV), elevated RC (1.77 mmol/L), low ALI, multiple tumors, large tumor size, elevated AFP, and major resection were among the key factors positively driving the prediction (Figure 5C). Conversely, in a low-risk patient (Predicted risk score: 113), factors such as early TNM stage (I+II), RC = 1.18 mmol/L, solitary tumor, and absence of vascular invasion contributed negatively to the risk prediction, reducing the base risk value (Figure 5D). These explanations enhance clinical transparency by illustrating how each feature influences individual outcome predictions, thereby supporting potential integration into clinical decision-making processes.

Model Deployment and Clinical Application

To facilitate the practical use of our prognostic model by clinicians, researchers, patients, and their families, we developed an interactive web-based prediction tool. This tool allows users to input individual patient parameters and obtain personalized survival risk assessments based on the XGBoost model. The application is publicly accessible and can be visited at: https://liugaom.shinyapps.io/XGBOOST_OS/.

Discussion

This study identified a significant non-linear relationship between RC levels and overall survival in patients with HCC after hepatectomy. We found that both excessively low and high RC levels were associated with increased mortality risk, exhibiting a U-shaped association with the lowest risk observed at RC levels around 1.04 mmol/L. Furthermore, we developed and validated a machine learning-based predictive model that incorporates RC along with established clinicopathological variables, demonstrating high prognostic accuracy and clinical utility.

HCC progression involves complex interactions between metabolic dysregulation, inflammation, and tumor microenvironment alterations.[19] Previous studies have established that lipid metabolism abnormalities play crucial roles in hepatocarcinogenesis and tumor progression.[20,21] Cholesterol, as an essential lipid component, participates in multiple biological processes including cell membrane construction, hormone synthesis, and signal transduction. Dysregulation of cholesterol homeostasis has been observed in various pathological conditions, including liver diseases, metabolic disorders, and multiple cancer types.[22]

Unlike previous studies that primarily focused on conventional lipid parameters (such as total cholesterol, HDL, LDL, and triglycerides),[23,24] our investigation highlights the particular significance of RC - the cholesterol content of triglyceride-rich lipoproteins including VLDL, IDL, and chylomicron remnants. RC has recently garnered increasing attention in cardiovascular and metabolic diseases including metabolic dysfunction-associated steatotic liver disease,[25–27] but its role in cancer prognosis remains largely unexplored. Our findings suggest that RC may represent a sensitive prognostic indicator of metabolic dysregulation in HCC patients.

Building upon this emerging relevance, our findings reveal a U-shaped relationship between RC and OS in HCC, suggesting that RC levels may reflect the body's metabolic balance. Moderate RC levels represent an appropriate state of cholesterol metabolism and are essential for maintaining cellular membrane integrity, hormone synthesis, and energy metabolism.[28] In contrast, deviations from the optimal RC range likely trigger distinct pathogenic cascades. At the lower extreme, very low RC levels are often a marker of profound malnutrition and impaired hepatic synthetic function.[29,30] This energy-deficient state can compromise immune cell function, weaken anti-tumor immunity, and critically impair the liver's regenerative capacity post-resection. For instance, cholesterol deficiency can disrupt T cell metabolism, particularly in CD8+ T cells, through the downregulation of the SREBP2 pathway and concomitant upregulation of the LXR pathway, which induces autophagy-mediated apoptosis and exacerbates T cell exhaustion.[4] Inhibiting the AXL-NPC1 signaling axis can enhance cholesterol mobilization, thereby improving the capacity of conventional dendritic cells (cDCs) to activate T cells and amplify anti-tumor immunity.[31] Furthermore, liver regeneration - a process dependent on growth factors like HGF secreted by immune cells such as macrophages - may be indirectly impaired by low cholesterol due to suppressed immune cell function and reduced release of regenerative factors.[32] On the other hand, elevated RC is an active contributor to tumor progression. Mechanistically, take Kupffer cells as example, high RC induces lipotoxicity and promotes chronic inflammation through the activation of pro-inflammatory pathways, such as the NLRP3-cGAS-STING axis, TNF-α-PPARα-EHBP1, and TLR4/NF-κB signaling, leading to upregulated expression of NLRP3 and inflammatory cytokines.[33–35] It directly fuels oncogenic signaling - including the HNF4A/ALDOB/AKT1 and CSNK2A1-IGF2R Ser2484 axes - by serving as a precursor for oxysterols that modulate cellular proliferation and metastasis.[36,37] The resulting dysregulated cholesterol metabolism, which often coexists with insulin resistance and disrupted bile acid/FXR signaling,[38,39] remodels the tumor microenvironment. This could occur via mechanisms such as SCAP/SREBP2 signaling dysregulation that restrains CD4+ T cell cytotoxicity and Liver X Receptor activity that shapes monocyte-to-DC differentiation, ultimately fostering an immunosuppressive niche that accelerates HCC progression.[40,41]

The synergistic prognostic effect observed between RC and ALI underscores profound biological and clinical implications. The poorest survival in patients with RC^{low} ALI^{low} exemplifies a "double-hit" scenario, where energy deprivation (low RC) synergizes with a systemic inflammatory and catabolic state (low ALI) to profoundly impair patient resilience and anti-tumor defense. Actually, similar synergistic prognostic effect could also be observed between RC and Child-Pugh score (data not shown). The best survival in patients with RC^{high} $Child^{low}$ suggests that in the context of preserved liver function ($Child^{low}$), higher RC levels may provide metabolic substrates necessary for recovery and immune defense without incurring significant lipotoxicity. This interplay was particularly critical in early-stage patients,

where metabolic and inflammatory factors may exert a greater relative impact on outcomes before advanced tumor biology dominates. Nevertheless, more studies are warranted on the interplay between RC and liver disease context, body composition parameters (such as muscle mass), and inflammatory markers.

Our machine learning approach further confirms the clinical value of RC in predicting HCC outcomes. The XGBoost model, which integrated RC with established prognostic factors, outperformed traditional statistical methods and other machine learning algorithms. It showed consistently higher accuracy in predicting survival over time and across patient subgroups. Moreover, the model effectively captured complex, non-linear interactions among risk variables. SHAP analysis provided clear and intuitive explanations for individual predictions, identifying RC as a key influential feature-alongside TNM stage and tumor characteristics. This interpretability builds clinical trust and supports practical use, offering a useful tool for personalized risk assessment and potential integration into routine care.

Translating these findings into clinical practice, it should be noted that preoperative RC measurement could serve as a valuable tool for risk stratification. For patients identified as high-risk - specifically those with RC levels outside the observed optimal range (0.59–2.74 mmol/L), which nevertheless requires further confirmation - tailored management strategies are warranted. This includes enhanced nutritional assessment and support for those with low RC to address underlying malnutrition, and aggressive management of associated metabolic comorbidities plus lifestyle interventions for those with markedly high RC. The high-risk patients should be considered for more intensive postoperative surveillance. Ultimately, future prospective studies are essential to explore whether actively modulating RC levels through dietary, pharmacological, or lifestyle interventions can improve survival outcomes.

Several limitations should be considered when interpreting our results. First, the single-center, retrospective nature of our study, conducted in an Asian region with a high prevalence of HBV, necessitates caution in generalizing the findings. The external validity of the identified RC optimal range and the machine learning model must be established in multicenter, larger sample prospective cohorts. This is particularly important for populations with differing predominant liver diseases (eg, metabolic dysfunction-associated steatotic liver disease or hepatitis C), ethnic backgrounds, and treatment landscapes, including those receiving novel systemic therapies, where cholesterol metabolism might have distinct roles. Second, RC was measured only at baseline, and dynamic changes during follow-up could provide additional prognostic information. Third, although we adjusted for numerous clinicopathological variables, unmeasured confounders such as genetic polymorphisms and detailed medication histories might still influence the observed associations. Forth, data of apo-B or VLDL-c was not available in most HCC patients in our center. However, direct measurements of these parameters but not indirect calculation of RC could provide additional granularity. Future prospective studies designed with these specific assays will be invaluable to confirm and refine our findings. Finally, the molecular mechanisms underlying the U-shaped relationship between RC and HCC survival warrant further investigation through basic and translational studies.

Despite these limitations, our findings have important clinical implications. The identification of an optimal RC range (0.59–2.74 mmol/L) provides a potential therapeutic target for nutritional and pharmacological interventions. The web-based prediction tool (https://liugaom.shinyapps.io/XGBOOST_OS/) offers a practical means for individualized risk assessment and treatment planning. Patients with RC levels outside the optimal range might benefit from closer monitoring and tailored management strategies.

Conclusions

In conclusion, our study demonstrates that RC exhibits a U-shaped relationship with overall survival in HCC patients after hepatectomy in an HBV-endemic, predominantly early-stage surgical cohort. By integrating RC with established prognostic factors through advanced machine learning approaches, we developed a predictive model with high accuracy and clinical interpretability. The identified observational optimal RC range provides a basis for understanding the importance of cholesterol metabolism in HCC. Future research should prioritize: (1) external validation such as in non-Asian cohorts, (2) exploration of RC's dynamic changes and clinical relevance, and (3) interventional trials evaluating whether nutritional or pharmacological modulation of RC improves survival outcomes.

Data Sharing Statement

Data sharing is not applicable to this article as all related data were reported in the manuscript and our hospital's policy.

Ethics Statement

The authors are accountable for all aspects of the work and ensure that questions related to the accuracy or integrity of any part of the work are appropriately investigated and resolved. The study was conducted by the Declaration of Helsinki (as revised in 2013). All protocols were approved by the Ethics and Indications Committee of the Meizhou People's Hospital (2023-C-95). The requirement for informed consent was waived for the retrospective study.

Funding

This work was supported by: The Guangdong Basic and Applied Basic Research Foundation, China (Grant No. 2023A1515220220); by the Training Program of the Scientific Research of Meizhou People's Hospital (Award Numbers PY-C2022038, PY-C2023040); by the Medical Scientific Research Foundation of Guangdong Province, China (Grant No. A2024679); and by the Meizhou Municipal Social Development Science and Technology Program (Project No. 2023C0301189).

Disclosure

The authors report no conflicts of interest in this work.

References

1. Bray F, Laversanne M, Sung H, et al. Global cancer statistics 2022: GLOBOCAN estimates of incidence and mortality worldwide for 36 cancers in 185 countries. *CA Cancer J Clin*. 2024;74:229–263. doi:10.3322/caac.21834
2. Dimitrios M, Alessandro M, Sarah S, et al. Advances in the treatment of hepatocellular carcinoma: an overview of the current and evolving therapeutic landscape for clinicians. *Cancer J Clin*. 2025.
3. Barcena-Varela M, Monga SP, Lujambio A. Precision models in hepatocellular carcinoma. *Nat Rev Gastroenterol Hepatol*. 2025;22(3):191–205.
4. Xiang J, Li Y, Mei S, et al. Novel diagnostic and therapeutic strategies based on PANoptosis for hepatocellular carcinoma. *Cancer Biol Med*. 2025;22(8):928–939. doi:10.20892/j.issn.2095-3941.2025.0150
5. Wenyao Z, Tomas G, Ralph RW, Wenbin LJACIEE. Multifunctional nanomaterials mediate cholesterol depletion for cancer treatment. *Angewandte Chemie*. 2024;136(46):e202412844.
6. Wan S, He Q-Y, Yang Y, et al. SPARC stabilizes ApoE to induce cholesterol-dependent invasion and sorafenib resistance in hepatocellular carcinoma. *Cancer Res*. 2024;84(11):1872–1888. doi:10.1158/0008-5472.CAN-23-2889
7. Fu R, Xue W, Liang J, et al. SOAT1 regulates cholesterol metabolism to induce EMT in hepatocellular carcinoma. *Cell Death Dis*. 2024;15(5):325. doi:10.1038/s41419-024-06711-9
8. Benjamin B, Richard T, Michael G, et al. Residual cholesterol and inflammatory risk in statin-treated patients undergoing percutaneous coronary intervention†. *Euro Heart J*. 2025:ehaf196.
9. Crudele L, De Matteis C, Piccinin E, et al. Low HDL-cholesterol levels predict hepatocellular carcinoma development in individuals with liver fibrosis. *JHEP Rep*. 2023;5(1):100627. doi:10.1016/j.jhepr.2022.100627
10. Li Z, Wang Y, Xing R, et al. Cholesterol efflux drives the generation of immunosuppressive macrophages to promote the progression of human hepatocellular carcinoma. *Cancer Immunol Res*. 2023;11(10):1400–1413. doi:10.1158/2326-6066.CIR-22-0907
11. Dai P, Feng J, Dong Y, et al. Metabolic reprogramming in hepatocellular carcinoma: an integrated omics study of lipid pathways and their diagnostic potential. *J Transl Med*. 2025;23(1):644. doi:10.1186/s12967-025-06698-7
12. He W, Wang M, Zhang X, et al. Estrogen induces LCAT to maintain cholesterol homeostasis and suppress hepatocellular carcinoma development. *Cancer Res*. 2024;84(15):2417–2431. doi:10.1158/0008-5472.CAN-23-3966
13. Han M, Huang K, Shen C, et al. Discordant high remnant cholesterol with LDL-C increases the risk of stroke: a chinese prospective cohort study. *Stroke*. 2024;55(8):2066–2074. doi:10.1161/STROKEAHA.124.046811
14. Gao Y, Hu Y, Xiang L. Remnant cholesterol, but not other cholesterol parameters, is associated with gestational diabetes mellitus in pregnant women: a prospective cohort study. *J Transl Med*. 2023;21(1):531. doi:10.1186/s12967-023-04322-0
15. Li Z, Yu C, Zhang H, et al. Impact of remnant cholesterol on short-term and long-term prognosis in patients with prediabetes or diabetes undergoing coronary artery bypass grafting: a large-scale cohort study. *Cardiovasc Diabetol*. 2025;24(1):8. doi:10.1186/s12933-024-02537-z
16. Shi J, Liu T, Liu C, et al. Remnant cholesterol is an effective biomarker for predicting survival in patients with breast cancer. *Nutr J*. 2024;23(1):45. doi:10.1186/s12937-024-00951-3
17. Tian Y, Wu Y, Qi M, et al. Associations of remnant cholesterol with cardiovascular and cancer mortality in a nationwide cohort. *Science Bulletin*. 2024;69(4):526–534. doi:10.1016/j.scib.2023.12.035
18. Vickers AJ, Elkin EB. EB E: decision curve analysis: a novel method for evaluating prediction models.%A Vickers AJ. *Med Decision Making*. 2006;26(6):565–574. doi:10.1177/0272989X06295361
19. Cheraghpour M, Hatami B, Singal AG. Lifestyle and pharmacologic approaches to prevention of metabolic dysfunction-associated steatotic liver disease-related hepatocellular carcinoma. *Clin Gastroenterol Hepatol*. 2025;23(5):685–694.e686. doi:10.1016/j.cgh.2024.09.041

20. Yang Y, Luo J, Wang Z, et al. Energy stress–induced circEPB41(2) promotes lipogenesis in hepatocellular carcinoma. *Cancer Res*. 2025;85 (4):723–738. doi:10.1158/0008-5472.CAN-24-1630
21. Yang X, Deng B, Zhao W, et al. FABP5+ lipid-loaded macrophages process tumour-derived unsaturated fatty acid signal to suppress T-cell antitumour immunity. *J Hepatol*. 2025;82(4):676–689. doi:10.1016/j.jhep.2024.09.029
22. Ziyi W, Xinyan L, Xiangyu SJBBARC. Targeting cholesterol metabolism in tumor and its immune microenvironment: opportunities and challenges. *Biochimica et Biophysica Acta*. 2025:189422.
23. Qianwei L, Dang W, Niklas H, et al. Lipids, apolipoproteins, carbohydrates, and risk of hematological malignancies. *Euro J Epidemiol*. 2025;40.
24. Su Youn N, Junwoo J, Won Kee L, Chang Min CJIJE. Factor modification in the association between high-density lipoprotein cholesterol and liver cancer risk in a nationwide cohort. *Inter J Epidemiol*. 2024;53(3):dyae053.
25. Kraaijenhof JM, Kerkvliet MJ, Nurmohamed NS, et al. The role of systemic inflammation in remnant cholesterol-associated cardiovascular risk: insights from the EPIC-Norfolk study. *Eur J Prev Cardiol*. 2025. doi:10.1093/eurjpc/zwaf037
26. Wadström BN, Borges MC, Wulff AB, et al. Elevated remnant and LDL cholesterol and the risk of peripheral artery disease: a Mendelian randomization study. *J Am Coll Cardiol*. 2025;85(12):1353–1368. doi:10.1016/j.jacc.2024.12.033
27. Miyake T, Furukawa S, Matsuura B, et al. Association between serum remnant cholesterol level and metabolic dysfunction-associated steatotic liver histology. *J Clin Endocrinol Metab*. 2025;110(6):e2064–e2070. doi:10.1210/clinem/dgae597
28. Sandra V, Marija T, Nemanja P, et al. The converging roles of microRNAs and lipid metabolism in atherosclerotic cardiovascular disease and cancer. In: *Seminars in Cancer Biology*. Academic Press; 2025:114.
29. Sharma V, Patial V. Insights into the molecular mechanisms of malnutrition-associated steatohepatitis: a review. *Liver Int*. 2024;44(9):2156–2173. doi:10.1111/liv.15932
30. Wei Y-S, Tang W-J, Mao P-Y, et al. Sexually dimorphic response to hepatic injury in newborn suffering from intrauterine growth restriction. *Adv Sci*. 2024;11(30):e2403095. doi:10.1002/advs.202403095
31. Meriem B, Matthew DP, Cédric MB, et al. Cholesterol mobilization regulates dendritic cell maturation and the immunogenic response to cancer. *Nat Immunol*. 2025;26(2):188–99.
32. Victoria B, Vanessa S, Samantha G, et al. Hepatectomy-induced apoptotic extracellular vesicles stimulate neutrophils to secrete regenerative growth factors. *J Hepatol*. 2022;77(6):1619–30.
33. Zhilei W, Jingwen L, Yu M, et al. Disruption of cholesterol homeostasis triggers NLRP3-cGAS-STING axis-dependent hepatic fibrosis and honokiol intervention effects. *Phytomedicine*. 2025:156904.
34. Yuxuan P, He C, Chang S, et al. Triclosan induces liver injury in long-life exposed mice via activation of TLR4/NF-κB/NLRP3 pathway. *Ecotoxicol Environ Safety*. 2024;273:116115.
35. Fanglin M, Miriam L, Marica M, et al. EHBP1 suppresses liver fibrosis in metabolic dysfunction-associated steatohepatitis. *Cell Metabol*. 2025;37 (5):1152–70.
36. Cai D, Zhong G-C, Dai X, et al. Targeting FDFT1 reduces cholesterol and bile acid production and delays hepatocellular carcinoma progression through the HNF4A/ALDOB/AKT1 axis. *Adv Sci*. 2025;12(12):e2411719. doi:10.1002/advs.202411719
37. Su R-Y, Xu C-H, Guo H-J, et al. Oncogenic cholesterol rewires lipid metabolism in hepatocellular carcinoma via the CSNK2A1-IGF2R Ser2484 axis. *J Adv Res*. 2025;76:449–465. doi:10.1016/j.jare.2024.11.021
38. Shimizu T, Miyoshi M, Kakinuma S, et al. Bile acid-FXR signaling facilitates the long-term maintenance of hepatic characteristics in human iPSC-derived organoids. *Cell Rep*. 2025;44(5):115675. doi:10.1016/j.celrep.2025.115675
39. Bansal SK, Bansal MB. Pathogenesis of MASLD and MASH - role of insulin resistance and lipotoxicity. *Aliment Pharmacol Ther*. 2024;59(Suppl 1): S10–s22.
40. Raccosta L, Marinozzi M, Costantini S, et al. Harnessing the reverse cholesterol transport pathway to favor differentiation of monocyte-derived APCs and antitumor responses. *Cell Death Dis*. 2023;14(2):129. doi:10.1038/s41419-023-05620-7
41. Wu M, Zhou X, Zhou X, et al. ZDHHC3-mediated SCAP S-acylation promotes cholesterol biosynthesis and tumor immune escape in hepatocellular carcinoma. *Cell Rep*. 2024;43(11):114962. doi:10.1016/j.celrep.2024.114962